crystals

MDPI

Communication

Crystal Structures of 3,3′,5,5′-Tetrabromo-4,4′-bipyridine and Co(II) Coordination Polymer Based Thereon

Ilyas F. Sakhapov [1,2], Almaz A. Zagidullin [2], Alexey B. Dobrynin [2], Igor A. Litvinov [2,3], Dmitry G. Yakhvarov [4], Mikhail A. Bondarenko [1,5], Alexander S. Novikov [6,7], Vladimir P. Fedin [5] and Sergey A. Adonin [1,5,8,*]

1 South Ural State University, 454080 Chelyabinsk, Russia
2 Arbuzov Institute of Organic and Physical Chemistry RAS, 420088 Kazan, Russia
3 A.N. Tupolev Kazan National Research Technical University, 420015 Kazan, Russia
4 Kazan Federal University, 420008 Kazan, Russia
5 Nikolaev Institute of Inorganic Chemistry SB RAS, 630090 Novosibirsk, Russia
6 Institute of Chemistry, Saint Petersburg University, 198504 Saint Petersburg, Russia
7 RUDN University, 117198 Moscow, Russia
8 Favorsky Irkutsk Institute of Chemistry SB RAS, 664033 Irkutsk, Russia
* Correspondence: adonin@niic.nsc.ru

Abstract: The crystal structure of 3,3′,5,5′-tetrabromo-4,4′-bipyridine (BrBipy, **1**) was determined, and the features of non-covalent interactions in solid state were investigated by theoretical methods. Using BrBipy as a linker ligand, 1D coordination polymer {[Co(BrBipy)$(NO_3)_2(CH_3OH)_2$]} (**2**) was obtained and characterized.

Keywords: non-covalent interactions; coordination polymers; halogen bonding; complexes; cobalt

check for updates

Citation: Sakhapov, I.F.; Zagidullin, A.A.; Dobrynin, A.B.; Litvinov, I.A.; Yakhvarov, D.G.; Bondarenko, M.A.; Novikov, A.S.; Fedin, V.P.; Adonin, S.A. Crystal Structures of 3,3′,5,5′-Tetrabromo-4,4′-bipyridine and Co(II) Coordination Polymer Based Thereon. *Crystals* **2023**, *13*, 704. https://doi.org/10.3390/cryst13040704

Academic Editor: Ulli Englert

Received: 27 March 2023
Revised: 6 April 2023
Accepted: 18 April 2023
Published: 20 April 2023

1. Introduction

Metal organic frameworks, or MOFs, have been intensively studied in recent decades [1–9] due to the wide range of their possible application areas, including chemistry and modern materials science. Those include (but are not limited to) selective separation of gases [10–14] and other substrates (usually organic, including isomers of xylene, benzene/cyclohexane etc. [8,15–18]), luminescent sensors [19–21], etc. The lion's share of MOFs are homo- or heterometallic carboxylates, mostly aromatic [22–24].

In this field, the most important role is probably played by the design of the linkers, which provides a diversity of possible non-covalent interactions with guest molecules in pores and, therefore, selectivity (of sorption, sensor recognition, etc.). Commonly, the most important contribution is given by hydrogen bonds, but in recent years there is a growing interest in MOFs in relation to building blocks able to form other, less conventional, non-covalent interactions, with halogen bonding (XB) a particular focus [25–27]. The number of articles focusing on this research is still quite low [28,29], but we assume that this area has great growth potential. Our suggestion is based on the fact that XB revealed itself as an efficient additional supramolecular "tool" that can be successfully utilized for "fine tuning" different physical and chemical properties of materials, including the abilities of highly selective binding and recognition (as an example, see numerous works by Beer et al. [30–34], which serve as a convincing illustration of this feature in sensor systems).

Very recently, we used DFT calculations to demonstrate that halogen-substituted derivatives of 4,4′-bipyridine (4,4′-bipy) are able to act as efficient XB donors [35]. Despite the fact that syntheses of numerous representatives of this class were described before [36,37], the number of corresponding MOFs based on them is very low—in our opinion undeservedly low. For bromo- and iodo-substituted bipys, the information about structurally characterized MOFs is limited to few homo- and heteroleptic Ag(I) complexes [38].

Moreover, the structures of many halogen-substituted bipys remain unknown, though they have been successfully synthesized and characterized by other physical methods (NMR etc.).

In this work, we decided to partially fill this gap. We determined the structure of 3,3′,5,5′-tetrabromo-4,4′-bipyridine (BrBipy) (**1**) and examined the features of non-covalent interactions in the crystalline state using theoretical methods. Additionally, we obtained coordination polymer based thereon—{[Co(Brbipy)$(NO_3)_2(CH_3OH)_2$]} (**2**).

2. Experimental Section

All chemicals were purchased from commercial sources (Brbipy precursors: Sigma-Aldrich, metal salts and solvents: ZAO Soyuzkhimprom (Russia)) and were used as purchased. The synthesis of Brbipy was based on the procedure described earlier [39]. The solvents were purified according to the standard methods. The crystals of **1** suitable for XRD were grown by dissolving **1** in chloroform and waiting for the consequent slow evaporation of the solvent.

2.1. Synthesis of **2**

$Co(NO_3)_2$ (0.12 g, 0.65 mmol) and BrBipy (0.63 mmol) were mixed with 22 mL of CH_3OH and stirred until complete dissolution. The mixture was then transferred into a flask, which was closed and kept at 100 °C for 48 h. Slow cooling of the solution resulted in purple crystals of **2** that were suitable for X-ray diffractometry. The yield was 60%. For $C_{12}H_{12}Br_4CoN_4O_8$ calcd, %: C, 20.15; H, 1.69; N, 7.84; found, %: C, 20.21; H, 1.74; N, 7.78.

2.2. X-ray Diffractometry

The XRD data were collected at 100K on a Bruker D8 QUEST with PHOTON II CCD diffractometer (Bruker AXS, Karlsruhe, Germany), using graphite monochromated MoKα (λ = 0.71073 Å) radiation and ω-scan rotation. Data collection images were indexed, integrated, and scaled using the APEX2 (**1**) or APEX3 (**2**) data reduction packages and corrected for absorption using SADABS software. The structures were solved by direct methods and refined using the SHELXT program [40]. All non-hydrogen atoms were refined anisotropically. H atoms were calculated on idealized positions and refined as riding atoms. Crystal data and refinement details are presented in Supplementary Materials. The data were deposited to the Cambridge Structural Database (2251626 and 2251676).

2.3. Powder X-ray Diffractometry

XRD analysis of polycrystals was performed on Shimadzu XRD-7000 diffractometer (CuK-alpha radiation, Ni—filter, linear One Sight detector, 0.0143° 2θ step, 2 s per step). Plotting of PXRD patterns and data treatment was performed using X'Pert Plus software (see Supplementary Materials).

2.4. Computational Details

The single point calculations based on the experimental X-ray geometries of **1** and **2** have been performed at the DFT level of theory using the dispersion-corrected hybrid functional ωB97XD [41] with the help of the Gaussian-09 program package. The 6-31+G* basis sets were used for all atoms. The topological analysis of the electron density distribution has been performed by using the Multiwfn program (version 3.7) [42]. The Cartesian atomic coordinates for model structures are presented in Supplementary Materials. The Hirshfeld surfaces analysis has been performed by using the CrystalExplorer program (version 17.5) [43]. The normalized contact distances (dnorm [44]) based on Bondi's van der Waals radii [45] were mapped into the Hirshfeld surfaces.

3. Results and Discussion

Compound **1** (see Figure 1) crystallizes in the triclinic space group. There are two independent Brbipy molecules in the crystal; the angles between the aromatic rings are close to 90° (84.56 and 86.11°, respectively). The crystal packing is presented in Figure 2.

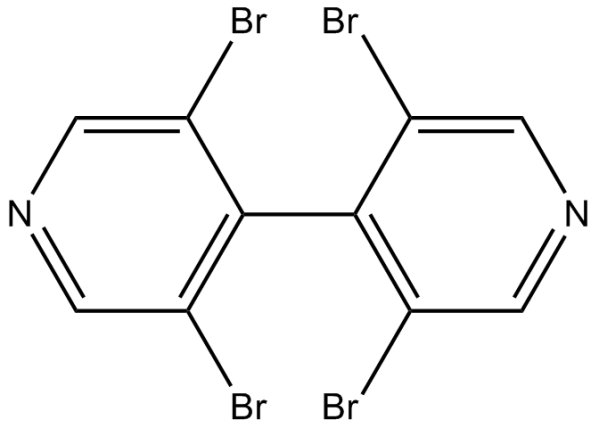

Figure 1. 3,3′,5,5′-tetrabromo-4,4′-bipyridine (BrBipy).

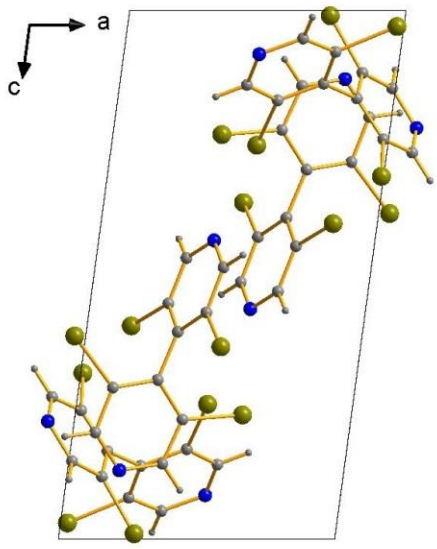

Figure 2. Crystal packing in the structure of **1**. Here and below: C and H grey, N deep blue, Br olive-green.

A comparison of N· · · Br distances with the sum of corresponding Bondi's van der Waal radii (S_w, 3.38 Å [45,46]) indicates the possible presence of non-covalent interactions, but their systems are different for two non-equivalent Brbipy units. The XB involves either only one N atom and two Br atoms of another aromatic ring or else both N and one Br atoms (Figure 3), respectively. The N· · · Br are 3.088, 3.150, and 3.160 Å (91.3, 93.2 and 93.5% of S_w, respectively). It can also be assumed that there are Br· · · Br interactions (S_w = 3.66 Å) of two types (Figure 4; 3.459 and 3.603 Å, respectively). Interestingly, the overall system of non-covalent interactions results in the assembly of a 3D supramolecular structure that is porous.

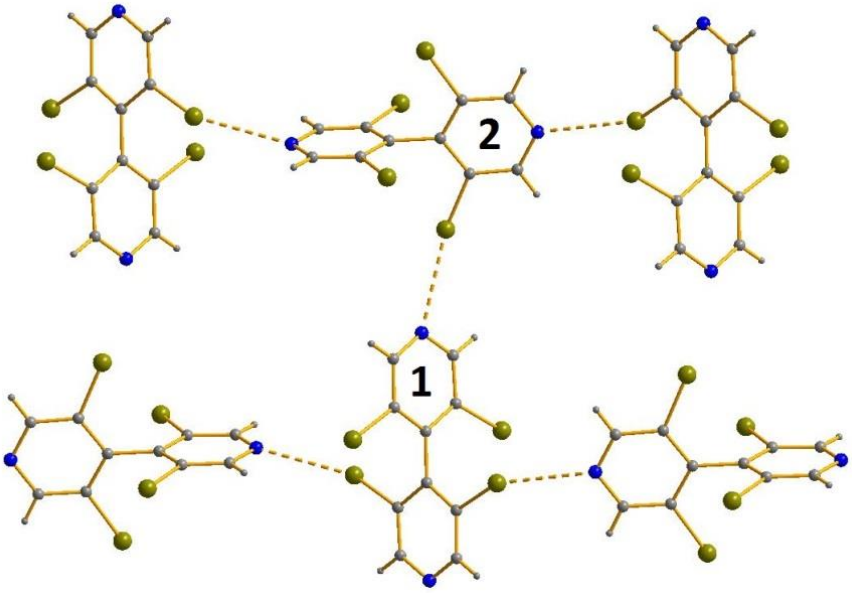

Figure 3. The system of N· · · Br interactions (dashed) in **1**.

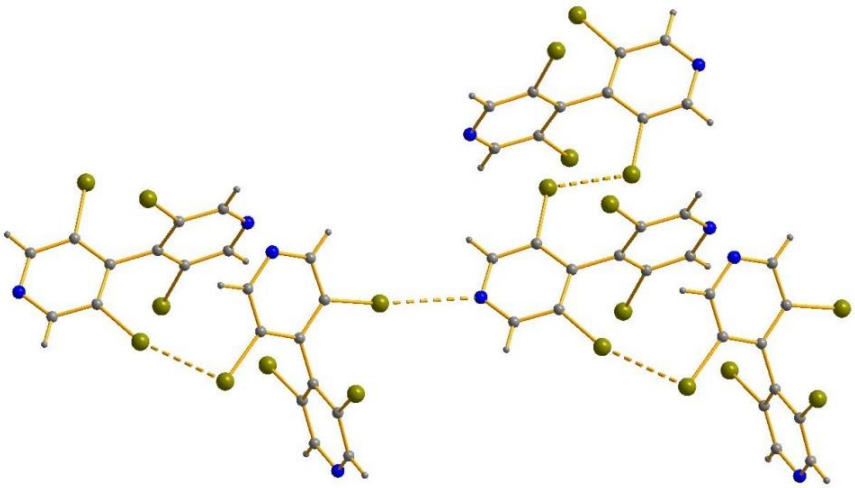

Figure 4. The system of Br· · · Br interactions (dashed) in **1**.

Previously, only one XRD dataset for 3,3′,5,5′-tetrahalo-4,4′-bipyridine (3-bromo-3′-iodo,5-bromo-5′-iodo) was described [47]. In this case, the cell parameters are very similar to those in **1**, so it can be regarded as isostructural, but the system of hypothetic non-covalent interactions is more sophisticated due to Br/I disordering. The structures of the other halogen-substituted derivatives of 4,4′-bipy, such as 2,2′,3,3′,5,5′-hexabromo- [48], also feature numerous N· · · X and X· · · X interactions.

In the structure of **2**, Co(II) metal centers have ordinary slightly distorted (L-Co-L = 86.49–93.51°) octahedral geometry. The coordination environment consists of two CH_3OH (Co-O = 2.074 Å), two nitrate (Co-O = 2.098 Å), and two BrBipy ligands (Co-N = 2.120–2.200 Å). The latter connect Co(II) into one-dimensional coordination polymer (Figure 5). Interestingly, the angle between the aromatic rings of Brbipy is slightly different (82.78°) from those found in pure **1**. There are also Br· · · O interactions, which can be regarded as halogen bonds (3.146 and 3.289 Å; S_w = 3.35 Å) connecting all Br atoms of Brbipy with nitrate ligands of neighboring coordination chains (Figure 6) to give an extended supramolecular motif. Unfortunately, our primary attempts to prepare coordination polymer of greater dimensionality (including 3D MOFs, which are particular cases of coordination polymers we aimed to prepare) by adding carboxylate (terephthalate, isophthalate,

etc.) linkers to the reaction mixture did not give any crystals suitable for characterization by diffraction techniques. However, we do not exclude the possibility of preparation of such compounds in the future.

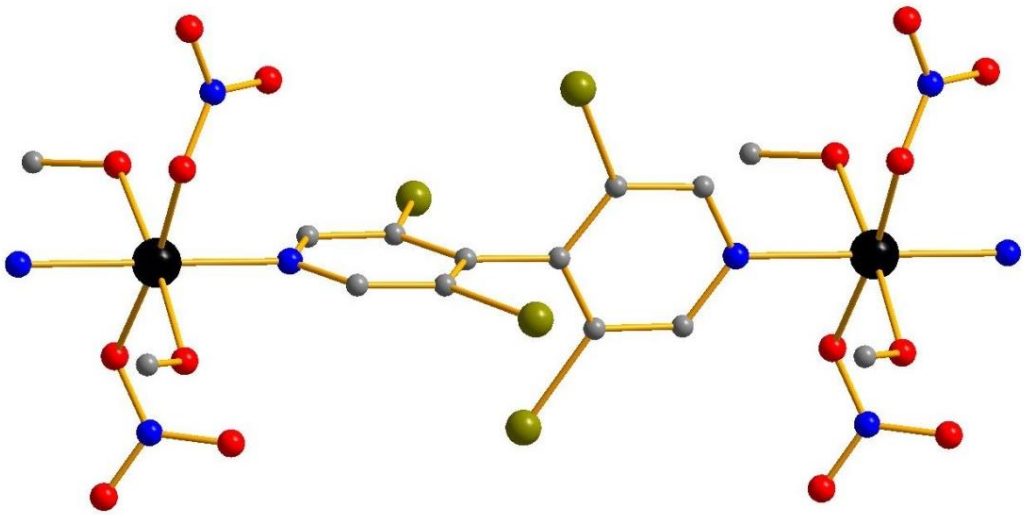

Figure 5. Fragment of the structure of **2**. H atoms are omitted from clarity; only N atoms of side Brbipy ligands are shown. Co black, O red.

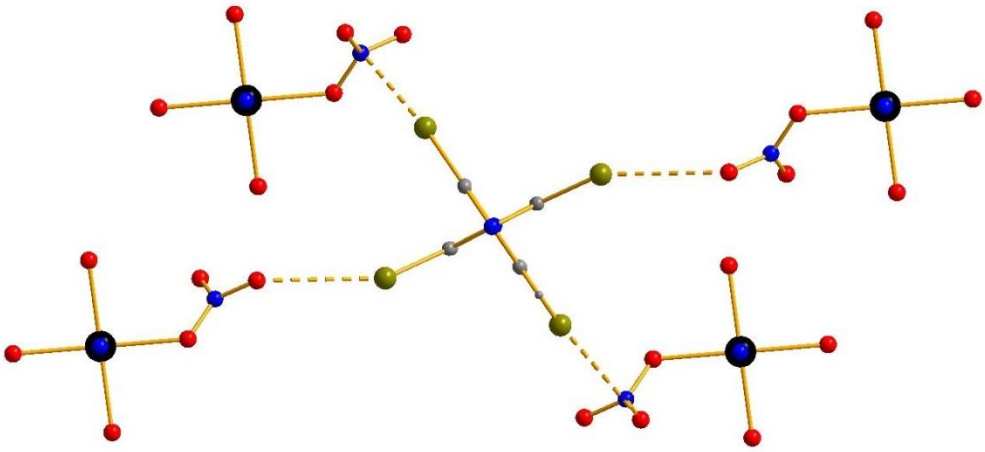

Figure 6. Br· · · O interactions in the structure of **2**.

As mentioned above, **2** represents the first case of a coordination polymer based on Br- or I-substituted derivatives of 4,4′-bipy with metal other than Ag(I), which makes direct comparison of its structure with previously reported ones rather problematic. However, there are numerous examples of complexes bearing $\{Co(NO_3)_2\}$ unit as well as other bipy derivatives (in 1:1 or 1:2 ratio) featuring one- or two-dimensional geometry [49–53]. The key bond lengths in these structures are, in general, similar to those found in **2**.

The element analysis data agree very well with theoretically calculated values. Interestingly, the powder X-ray diffractometry data indicate some impurities (there are the target phases and some by-products), which, in our opinion, can be polymorphs.

To examine the nature and approximately estimate the energies of halogen bonds Br· · · N, Br· · · Br and Br· · · O in **1** and **2**, we performed DFT calculations as well as the topological analysis of the electron density distribution (ωB97XD/6-31+G*, see Computational details and Supplementary Materials) for model structures. Results are summarized in Table 1; visualization for halogen bonds Br· · · N, Br· · · Br and Br· · · O in **1** and **2** is shown in Supplementary Materials.

Table 1. Values of the density of all electrons—ρ(**r**), Laplacian of electron density—$\nabla^2\rho$(**r**) and appropriate λ_2 eigenvalues, energy density—H_b, potential energy density—V(**r**), Lagrangian kinetic energy—G(**r**), and electron localization function—ELF (a.u.) at the bond critical points (3, −1), corresponding to halogen bonds Br···N, Br···Br and Br···O in **1** and **2**, and estimated strength for these interactions E_{int} (kcal/mol).

Contact *	ρ(r)	$\nabla^2\rho$(r)	λ_2	H_b	V(r)	G(r)	ELF	E_{int} **
			1					
Br···N 3.088 Å	0.012	0.040	−0.012	0.002	−0.007	0.009	0.048	2.5
Br···N 3.150 Å	0.011	0.036	−0.011	0.002	−0.006	0.008	0.046	2.2
Br···N 3.160 Å	0.011	0.034	−0.011	0.001	−0.006	0.007	0.041	2.2
Br···Br 3.459 Å	0.010	0.032	−0.010	0.001	−0.005	0.006	0.040	1.8
			2					
Br···O 3.146 Å	0.009	0.031	−0.009	0.002	−0.005	0.007	0.024	1.8
Br···O 3.290 Å	0.007	0.024	−0.007	0.001	−0.004	0.005	0.017	1.5

* The Bondi's van der Waals radii for Br, N, and O atoms are 1.83, 1.55, and 1.52 Å. ** E_{int} = 0.58(−V(**r**)) (this correlation between the interaction energy and the potential energy density of electrons at the bond critical points (3, −1) was specifically developed for halogen bonds involving bromine atoms [54]).

The QTAIM analysis of the model structures (coordinates of atoms were taken from XRD data and used "as is", i.e., without optimization of geometry) indicates that there are bond critical points (3, −1) for halogen bonds Br···N, Br···Br and Br···O in **1** and **2**, respectively. The key characteristics (magnitude of the electron density (0.004–0.012 a.u.), values of the Laplacian of electron density (0.011–0.040 a.u.), energy density (0.000–0.002 a.u.), and values of electron localization function (0.014–0.048 a.u.)) in these bond critical points (3, −1), as well as the energies of examined contacts (0.7–2.5 kcal/mol), are quite usual for noncovalent interactions involving bromine atoms in similar chemical systems. As follows from the analysis of the balance between G(**r**) and V(**r**) at the bond critical points (3, −1) for halogen bonds Br···N, Br···Br and Br···O in **1** and **2** (viz. $-G(\mathbf{r})/V(\mathbf{r}) \geq 1$), the covalent contribution in these interactions is negligible [55]. The sign of λ_2 can be used to see whether the interaction is bonding or nonvonding [56,57]; in all cases examined within this study, the halogen bonds Br···N, Br···Br and Br···O are attractive.

To see which sort of interatomic interaction gives the major contributions in the formation of crystal packing, we performed Hirshfeld surface analysis for the X-ray structures **1** and **2** (Table 2, Figure 7). These data demonstrate that in both cases, crystal packing is determined predominantly by interatomic contacts of Br–H type.

Table 2. Main partial contributions of different interatomic contacts to the Hirshfeld surfaces of X-ray structures **1** and **2**.

Structure	Contributions of Different Interatomic Contacts to the Hirshfeld Surfaces
1	Br–H 34.2%, Br–Br 17.6%, N–H 11.1%, Br–C 10.9%, Br–N 8.3%, C–H 7.1%, H–H 6.3%, N–C 2.5%, C–C 1.9%
2	Br–H 31.2%, O–H 23.3%, Br–O 11.6%, H–H 9.7%, Br–Br 7.0%, Br–C 5.4%, C–H 3.0%, O–C 2.3%, Br–N 1.9%, O–N 1.4%, Co–N 1.3%, N–H 1.1%, O–O 0.5%, Co–H 0.1%

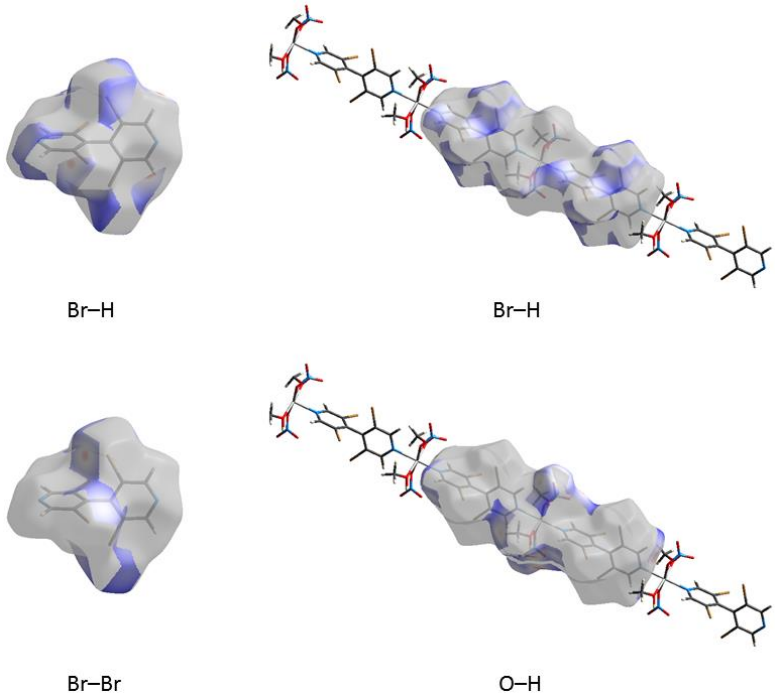

Figure 7. Visualization of Hirshfeld surfaces showing most dominated interatomic contacts in the X-ray structures **1** (**left**) and **2** (**right**).

4. Conclusions

To conclude, we demonstrated that bromine-substituted derivatives of 4,4′-bipyridine can, on the one hand, be regarded as promising building blocks for design of supramolecular systems based on halogen bond formation, and, on the other, they can, as expected, act as linkers for the design of coordination polymers. However, we isolated only one example, and it is one-dimensional, but we can nonetheless expect that other geometries, including porous 3D MOFs, can be achieved in further compounds of this family. Corresponding experiments are underway in our group.

Supplementary Materials: The following supporting information can be downloaded at: https://www.mdpi.com/article/10.3390/cryst13040704/s1, details of XRD and PXRD experiments as well as computational details.

Author Contributions: Conceptualization, S.A.A. and V.P.F.; methodology, S.A.A. and V.P.F.; validation, S.A.A., A.A.Z. and D.G.Y.; formal analysis, I.A.L. and A.S.N.; investigation, I.F.S., A.A.Z., I.A.L., A.S.N. and A.B.D.; resources, S.A.A. and D.G.Y.; data curation, M.A.B. and I.F.S.; writing—original draft preparation, S.A.A. and A.S.N.; writing—review and editing, S.A.A.; visualization, A.S.N., S.A.A. and A.B.D.; supervision, S.A.A.; project administration, S.A.A. and D.G.Y.; funding acquisition, S.A.A. All authors have read and agreed to the published version of the manuscript.

Funding: This research was funded by Russian Science Foundation, Grant No. 21-73-20019, and partially supported by Ministry of Science and Higher Education of the Russian Federation (examination of the sorption properties of the samples, 121031700313-8). A.S.N. thanks RUDN University Strategic Academic Leadership Program (DFT calculations and Hirshfeld Surface Analysis).

Institutional Review Board Statement: Not applicable.

Informed Consent Statement: Not applicable.

Acknowledgments: The authors thank the Resource center of Saint Petersburg State University for assistance in preliminary (screening) XRD experiments.

Conflicts of Interest: The authors declare no conflict of interest.

References

1. Li, B.; Wen, H.-M.; Cui, Y.; Zhou, W.; Qian, G.; Chen, B. Emerging Multifunctional Metal–Organic Framework Materials. *Adv. Mater.* **2016**, *28*, 8819–8860. [CrossRef]
2. Andreichenko, A.A.; Burlak, P.V.; Kovalenko, K.A.; Samsonenko, D.G.; Fedin, V.P. Zinc(II) and Cadmium(II) Metal-Organic Frameworks Based on the Amide-Functionalized Tetracarboxylate Ligand: Synthesis, Crystal Structure, and Luminescent Properties. *J. Struct. Chem.* **2022**, *63*, 378–387. [CrossRef]
3. Kiraev, S.R.; Nikolaevskii, S.A.; Kiskin, M.A.; Ananyev, I.V.; Varaksina, E.A.; Taydakov, I.V.; Aleksandrov, G.G.; Goloveshkin, A.S.; Sidorov, A.A.; Lyssenko, K.A.; et al. Synthesis, structure and photoluminescence properties of $\{Zn_2Ln_2\}$ heterometallic complexes with anions of 1-naphthylacetic acid and N-donor heterocyclic ligands. *Inorg. Chim. Acta* **2018**, *477*, 15–23. [CrossRef]
4. Primakov, P.V.; Denisov, G.L.; Novikov, V.V.; Lependina, O.L.; Korlyukov, A.A.; Nelyubina, Y.V. Calcium-based coordination polymers from a solvothermal synthesis of HKUST-1 in 3D printed autoclaves. *Mendeleev Commun.* **2022**, *32*, 105–108. [CrossRef]
5. Li, G.-L.; Yin, W.-D.; Zhang, J.-Y.; Du, G.-J.; Xia, Y.-H.; Liu, G.-Z. A 3D Zn(II) Metal-Organic Framework Based on Citraconic Acid and 1,2-Bi(4-pyridyl)ethylene Mixed Ligands: Crystal Structure, Luminescence, and [2 + 2] Cycloaddition Reaction. *Russ. J. Inorg. Chem.* **2022**, *67*, 1745–1750.
6. Guo, L.-D.; Zhao, X.-H.; Liu, Y.-Y.; Zuo, X.-R.; Yao, J.; Sun, J.-R.; Xu, D.-M.; Li, F.-P.; Li, W.-H. In Situ Ligand Synthesis Afforded Two New Metal-Organic Compounds: Luminescent and Photocatalytic Properties. *Russ. J. Inorg. Chem.* **2022**, *67*, 2140–2147. [CrossRef]
7. Zhang, X.; Da Silva, I.; Fazzi, R.; Sheveleva, A.M.; Han, X.; Spencer, B.F.; Sapchenko, S.A.; Tuna, F.; McInnes, E.J.L.; Li, M.; et al. Iodine Adsorption in a Redox-Active Metal-Organic Framework: Electrical Conductivity Induced by Host-Guest Charge-Transfer. *Inorg. Chem.* **2019**, *58*, 14145–14150. [CrossRef] [PubMed]
8. Li, J.; Han, X.; Kang, X.; Chen, Y.; Xu, S.; Smith, G.L.; Tillotson, E.; Cheng, Y.; McCormick McPherson, L.J.; Teat, S.J.; et al. Purification of Propylene and Ethylene by a Robust Metal–Organic Framework Mediated by Host–Guest Interactions. *Angew. Chem. Int. Ed.* **2021**, *60*, 15541–15547. [CrossRef]
9. Schoedel, A.; Li, M.; Li, D.; O'Keeffe, M.; Yaghi, O.M. Structures of Metal-Organic Frameworks with Rod Secondary Building Units. *Chem. Rev.* **2016**, *116*, 12466–12535. [CrossRef]
10. Sapianik, A.A.; Dudko, E.R.; Kovalenko, K.A.; Barsukova, M.O.; Samsonenko, D.G.; Dybtsev, D.N.; Fedin, V.P. Metal-Organic Frameworks for Highly Selective Separation of Xylene Isomers and Single-Crystal X-ray Study of Aromatic Guest-Host Inclusion Compounds. *ACS Appl. Mater. Interfaces* **2021**, *13*, 14768–14777. [CrossRef]
11. Xu, N.; Hu, J.; Wang, L.; Luo, D.; Sun, W.; Hu, Y.; Wang, D.; Cui, X.; Xing, H.; Zhang, Y. A TIFSIX pillared MOF with unprecedented zsd topology for efficient separation of acetylene from quaternary mixtures. *Chem. Eng. J.* **2022**, *450*, 138034. [CrossRef]
12. Pal, A.; Lin, J.-B.; Chand, S.; Das, M.C. A 3D Microporous MOF with mab Topology for Selective CO_2 Adsorption and Separation. *ChemistrySelect* **2018**, *3*, 917–921. [CrossRef]
13. Pal, S.C.; Ahmed, R.; Manna, A.K.; Das, M.C. Potential of a pH-Stable Microporous MOF for C_2H_2/C_2H_4 and C_2H_2/CO_2 Gas Separations under Ambient Conditions. *Inorg. Chem.* **2022**, *61*, 18293–18302. [CrossRef]
14. Pal, A.; Chand, S.; Elahi, S.M.; Das, M.C. A microporous MOF with a polar pore surface exhibiting excellent selective adsorption of CO_2 from CO_2-N_2 and CO_2-CH_4 gas mixtures with high CO_2 loading. *Dalt. Trans.* **2017**, *46*, 15280–15286. [CrossRef] [PubMed]
15. Sapianik, A.A.; Kovalenko, K.A.; Samsonenko, D.G.; Barsukova, M.O.; Dybtsev, D.N.; Fedin, V.P. Exceptionally effective benzene/cyclohexane separation using a nitro-decorated metal-organic framework. *Chem. Commun.* **2020**, *56*, 8241–8244. [CrossRef]
16. Trenholme, W.J.F.; Kolokolov, D.I.; Bound, M.; Argent, S.P.; Gould, J.A.; Li, J.; Barnett, S.A.; Blake, A.J.; Stepanov, A.G.; Besley, E.; et al. Selective Gas Uptake and Rotational Dynamics in a (3,24)-Connected Metal-Organic Framework Material. *J. Am. Chem. Soc.* **2021**, *143*, 3348–3358. [CrossRef]
17. Ji, G.-J.; Xiang, T.; Zhou, X.-Q.; Chen, L.; Zhang, Z.-H.; Lu, B.-B.; Zhou, X.-J. Molecular dynamics simulation of adsorption and separation of xylene isomers by Cu-HKUST-1. *RSC Adv.* **2022**, *12*, 35290–35299. [CrossRef]
18. Zheng, X.; Rehman, S.; Zhang, P. Room temperature synthesis of monolithic MIL-100(Fe) in aqueous solution for energy-efficient removal and recovery of aromatic volatile organic compounds. *J. Hazard. Mater.* **2023**, *442*, 129998. [CrossRef] [PubMed]
19. Pavlov, D.I.; Sukhikh, T.S.; Ryadun, A.A.; Matveevskaya, V.V.; Kovalenko, K.A.; Benassi, E.; Fedin, V.P.; Potapov, A.S. A luminescent 2,1,3-benzoxadiazole-decorated zirconium-organic framework as an exceptionally sensitive turn-on sensor for ammonia and aliphatic amines in water. *J. Mater. Chem. C* **2022**, *10*, 5567–5575. [CrossRef]
20. Xia, T.; Jiang, L.; Zhang, J.; Wan, Y.; Yang, Y.; Gan, J.; Cui, Y.; Yang, Z.; Qian, G. A fluorometric metal-organic framework oxygen sensor: From sensitive powder to portable optical fiber device. *Microporous Mesoporous Mater.* **2020**, *305*, 110396. [CrossRef]
21. Cui, Y.; Yue, D.; Huang, Y.; Zhang, J.; Wang, Z.; Yang, D.; Qian, G. Photo-induced electron transfer in a metal-organic framework: A new approach towards a highly sensitive luminescent probe for Fe^{3+}. *Chem. Commun.* **2019**, *55*, 11231–11234. [CrossRef]
22. Zorina-Tikhonova, E.N.; Yambulatov, D.S.; Kiskin, M.A.; Bazhina, E.S.; Nikolaevskii, S.A.; Gogoleva, N.V.; Lutsenko, I.A.; Sidorov, A.A.; Eremenko, I.L. Synthesis and Structure of New Polymeric Lithium Pivalates. *Russ. J. Coord. Chem.* **2020**, *46*, 75–80. [CrossRef]
23. Yashkova, K.A.; Mel'nikov, S.N.; Nikolaevskii, S.A.; Shmelev, M.A.; Sidorov, A.A.; Kiskin, M.A.; Eremenko, I.L. Synthesis and Structure of an Nontrivial Coordination Polymer $\{[Na_2Co(pfb)_2(H_2O)_8](pfb)_2\}_n$ with Pentafluorobenzoate Anions. *J. Struct. Chem.* **2021**, *62*, 1378–1384. [CrossRef]

24. Kolokolov, F.A.; Kulyasov, A.N.; Magomadova, M.A.; Shapieva, K.K.; Mikhailov, I.E.; Dushenko, G.A.; Panyushkin, V.A. Synthesis and luminescent properties of coordination compounds of europium(III), gadolinium(III), and terbium(III) with para-alkyloxybenzoic acids. *Russ. J. Gen. Chem.* **2016**, *86*, 1209–1211. [CrossRef]
25. Eliseeva, A.A.; Ivanov, D.M.; Novikov, A.S.; Kukushkin, V.Y. Recognition of the π-hole donor ability of iodopentafluorobenzene-a conventional σ-hole donor for crystal engineering involving halogen bonding. *CrystEngComm* **2019**, *21*, 616–628. [CrossRef]
26. Eliseeva, A.A.; Ivanov, D.M.; Novikov, A.S.; Rozhkov, A.V.; Kornyakov, I.V.; Dubovtsev, A.Y.; Kukushkin, V.Y. Hexaiododiplatinate(ii) as a useful supramolecular synthon for halogen bond involving crystal engineering. *Dalt. Trans.* **2020**, *49*, 356–367. [CrossRef] [PubMed]
27. Awwadi, F.F.; Taher, D.; Haddad, S.F.; Turnbull, M.M. Competition between Hydrogen and Halogen Bonding Interactions: Theoretical and Crystallographic Studies. *Cryst. Growth Des.* **2014**, *14*, 1961–1971. [CrossRef]
28. Kalaj, M.; Momeni, M.R.; Bentz, K.C.; Barcus, K.S.; Palomba, J.M.; Paesani, F.; Cohen, S.M. Halogen bonding in UiO-66 frameworks promotes superior chemical warfare agent simulant degradation. *Chem. Commun.* **2019**, *55*, 3481–3484. [CrossRef] [PubMed]
29. Li, B.; Dong, M.-M.; Fan, H.-T.; Feng, C.-Q.; Zang, S.-Q.; Wang, L.-Y. Halogen···halogen interactions in the assembly of high-dimensional supramolecular coordination polymers based on 3,5-diiodobenzoic acid. *Cryst. Growth Des.* **2014**, *14*, 6325–6336. [CrossRef]
30. Gilday, L.C.; Robinson, S.W.; Barendt, T.A.; Langton, M.J.; Mullaney, B.R.; Beer, P.D. Halogen Bonding in Supramolecular Chemistry. *Chem. Rev.* **2015**, *115*, 7118–7195. [CrossRef]
31. Mullaney, B.R.; Thompson, A.L.; Beer, P.D. An All-Halogen Bonding Rotaxane for Selective Sensing of Halides in Aqueous Media. *Angew. Chem. Int. Ed.* **2014**, *53*, 11458–11462. [CrossRef] [PubMed]
32. Hein, R.; Borissov, A.; Smith, M.D.; Beer, P.D.; Davis, J.J. A halogen-bonding foldamer molecular film for selective reagentless anion sensing in water. *Chem. Commun.* **2019**, *55*, 4849–4852. [CrossRef] [PubMed]
33. Bunchuay, T.; Docker, A.; White, N.G.; Beer, P.D. A new halogen bonding 1,2-iodo-triazolium-triazole benzene motif for anion recognition. *Polyhedron* **2021**, *209*, 115482. [CrossRef]
34. Bunchuay, T.; Boonpalit, K.; Docker, A.; Ruengsuk, A.; Tantirungrotechai, J.; Sukwattanasinitt, M.; Surawatanawong, P.; Beer, P.D. Charge neutral halogen bonding tetradentate-iodotriazole macrocycles capable of anion recognition and sensing in highly competitive aqueous media. *Chem. Commun.* **2021**, *57*, 11976–11979. [CrossRef]
35. Novikov, A.S.; Sakhapov, I.F.; Zaguzin, A.S.; Fedin, V.P.; Adonin, S.A. Halogen Bond in Porous Materials: Rational Selection of Building Blocks. *J. Struct. Chem.* **2022**, *63*, 1880–1886. [CrossRef]
36. Lee, D.A.; Peloquin, D.M.; Yapi, E.W.; McMinn, L.A.; Merkert, J.W.; Donovan-Merkert, B.T.; Vitallo, A.A.; Peterson, A.R.; Jones, D.S.; Ceccarelli, C.; et al. "Tetramethylsilanoviologen": Synthesis, characterization, and hydrolysis of a Silolodipyridinium ion. *Polyhedron* **2017**, *133*, 358–363. [CrossRef]
37. Richard, J.; Joseph, J.; Wang, C.; Ciesielski, A.; Weiss, J.; Samorì, P.; Mamane, V.; Wytko, J.A. Functionalized 4,4′-Bipyridines: Synthesis and 2D Organization on Highly Oriented Pyrolytic Graphite. *J. Org. Chem.* **2021**, *86*, 3356–3366. [CrossRef]
38. Aubert, E.; Abboud, M.; Doudouh, A.; Durand, P.; Peluso, P.; Ligresti, A.; Vigolo, B.; Cossu, S.; Pale, P.; Mamane, V. Silver(i) coordination polymers with 3,3′,5,5′-tetrasubstituted 4,4′-bipyridine ligands: Towards new porous chiral materials. *RSC Adv.* **2017**, *7*, 7358–7367. [CrossRef]
39. Abboud, M.; Mamane, V.; Aubert, E.; Lecomte, C.; Fort, Y. Synthesis of polyhalogenated 4,4′-bipyridines via a simple dimerization procedure. *J. Org. Chem.* **2010**, *75*, 3224–3231. [CrossRef]
40. Sheldrick, G.M. SHELXT—Integrated space-group and crystal-structure determination. *Acta Crystallogr. Sect. A Found. Adv.* **2015**, *71*, 3–8. [CrossRef]
41. Chai, J.D.; Head-Gordon, M. Long-range corrected hybrid density functionals with damped atom-atom dispersion corrections. *Phys. Chem. Chem. Phys.* **2008**, *10*, 6615–6620. [CrossRef]
42. Lu, T.; Chen, F. Multiwfn: A multifunctional wavefunction analyzer. *J. Comput. Chem.* **2012**, *33*, 580–592. [CrossRef] [PubMed]
43. Turner, M.J.; Mckinnon, J.J.; Wolff, S.K.; Grimwood, D.J.; Spackman, P.R.; Jayatilaka, D.S.; Spackman, M.A. *CrystalExplorer17*; University of Western Australia: Perth, Australia, 2017.
44. McKinnon, J.J.; Jayatilaka, D.; Spackman, M.A. Towards quantitative analysis of intermolecular interactions with Hirshfeld surfaces. *Chem. Commun.* **2007**, *37*, 3814–3816. [CrossRef]
45. Bondi, A. van der Waals Volumes and Radii of Metals in Covalent Compounds. *J. Phys. Chem.* **1966**, *70*, 3006–3007. [CrossRef]
46. Mantina, M.; Chamberlin, A.C.; Valero, R.; Cramer, C.J.; Truhlar, D.G. Consistent van der Waals radü for the whole main group. *J. Phys. Chem. A* **2009**, *113*, 5806–5812. [CrossRef] [PubMed]
47. Mamane, V.; Aubert, E.; Peluso, P.; Cossu, S. Synthesis, resolution, and absolute configuration of chiral 4,4′-bipyridines. *J. Org. Chem.* **2012**, *77*, 2579–2583. [CrossRef]
48. Mamane, V.; Peluso, P.; Aubert, E.; Cossu, S.; Pale, P. Chiral Hexahalogenated 4,4′-Bipyridines. *J. Org. Chem.* **2016**, *81*, 4576–4587. [CrossRef]
49. Felloni, M.; Blake, A.J.; Champness, N.R.; Hubberstey, P.; Wilson, C.; Schröder, M. Supramolecular interactions in 4,4′-bipyridine cobalt(II) nitrate networks. *J. Supramol. Chem.* **2002**, *2*, 163–174. [CrossRef]
50. Mauger-Sonnek, K.; Streicher, L.K.; Lamp, O.P.; Ellern, A.; Weeks, C.L. Structure control and sorption properties of porous coordination polymers prepared from M(NO3)2 and 4,4′-bipyridine (M = Co^{2+}, Ni^{2+}). *Inorg. Chim. Acta* **2014**, *418*, 73–83. [CrossRef]

51. Matsia, S.; Menelaou, M.; Hatzidimitriou, A.; Tangoulis, V.; Lalioti, N.; Ioannidis, N.; Blömer, L.; Kersting, B.; Salifoglou, A. Temperature-Sensitive Structural Speciation of Cobalt-Iminodialcohol-(N,N′-Aromatic Chelator) Systems: Lattice Architecture and Spectrochemical Properties. *Eur. J. Inorg. Chem.* **2020**, *2020*, 2919–2940. [CrossRef]
52. Halder, G.J.; Kepert, C.J. In situ single-crystal X-ray diffraction studies of desorption and sorption in a flexible nanoporous molecular framework material. *J. Am. Chem. Soc.* **2005**, *127*, 7891–7900. [CrossRef] [PubMed]
53. Kondo, M.; Yoshitomi, T.; Seki, K.; Matsuzaka, H.; Kitagawa, S. Three-Dimensional Framework with Channeling Cavities for Small Molecules: $\{[M_2(4,4'\text{-bpy})_3(NO_3)_4]\cdot xH_2O\}n$ (M = Co, Ni, Zn). *Angew. Chem.* **1997**, *36*, 1725–1727. [CrossRef]
54. Bartashevich, E.V.; Tsirelson, V.G. Interplay between non-covalent interactions in complexes and crystals with halogen bonds. *Russ. Chem. Rev.* **2014**, *83*, 1181–1203. [CrossRef]
55. Espinosa, E.; Alkorta, I.; Elguero, J.; Molins, E. From weak to strong interactions: A comprehensive analysis of the topological and energetic properties of the electron density distribution involving X–H$\cdots$F–Y systems. *J. Chem. Phys.* **2002**, *117*, 5529–5542. [CrossRef]
56. Johnson, E.R.; Keinan, S.; Mori-Sánchez, P.; Contreras-García, J.; Cohen, A.J.; Yang, W. Revealing Noncovalent Interactions. *J. Am. Chem. Soc.* **2010**, *132*, 6498–6506. [CrossRef]
57. Contreras-García, J.; Johnson, E.R.; Keinan, S.; Chaudret, R.; Piquemal, J.P.; Beratan, D.N.; Yang, W. NCIPLOT: A program for plotting noncovalent interaction regions. *J. Chem. Theory Comput.* **2011**, *7*, 625–632. [CrossRef] [PubMed]